Lagrangian Point Force regularization for dispersed two-phase flows

Jean-François Poustis, Jean-Mathieu Senoner, Philippe Villedieu

Lagrangian Point Force regularization for dispersed two-phase flows

Jean-François Poustis, Jean-Mathieu Senoner and Philippe Villedieu

ONERA/DMPE, University of Toulouse, F-31055 Toulouse, France

jean-francois.poustis@onera.fr, jean-mathieu.senoner@onera.fr and philippe.villedieu@onera.fr

Keywords: Euler-Lagrange, Statistical Lagrangian description, Diffusion Equation

Abstract

The present paper presents a regularization procedure of the Lagrangian point-particle approach for the simulation of dispersed two-phase flows in a statistical framework. The aim is to regularize the probability presence of a particle, written as a Dirac delta function centered on the particle position in the standard formulation, by a Gaussian like distribution. The associated regularization length scale is obtained by solving additional transport equations in the Lagrangian framework. The regularization itself is then achieved by solving two non-linear diffusion equations. The first diffusion equations allows to spread the field of spatially varying diffusion coefficients required for regularization over the computational mesh. Once this field is defined, regularization of the Lagrangian fields to be projected on the Eulerian grid such as particle density, particle velocity, etc... is performed. These ideas are then tested on simplified one-dimensional test cases. While preliminary results seem encouraging as the dispersed phase fields projected on the Eulerian grid appear much less sensitive to the initial sampling of the spray, further tests on more realistic test cases are necessary to conclude on precision gains with repect to the additional computational expense resulting from the regularization procedure.

1 Introduction

Dispersed two-phase flows are encountered in numerous natural phenomena and industrial applications such as spray combustion, spray coating or icing applications. The dispersed phase consists of a cloud of liquid or solid particles whose number is generally far too large to compute the evolution of each singe particle at a reasonable computational cost.

In order to reduce the computational cost, the dispersed phase may be described in a purely statistical sense using a probability density function (pdf). The evolution of this pdf follows Williams' equation (Williams 1958) and two main approaches can be used for its resolution: the Euler-Euler and the Euler-Lagrange approach. Both approaches have their advantages and drawbacks and the choice between them mainly depends on the target application.

In this work, the Euler-Lagrange approach is chosen. The fluid phase is described in a Eulerian framework while the dispersed phase is described by N numerical particles described by Lagrangian variables such as position, velocity, etc.... The fact that all particle properties are available at the particle scale generally makes the implementation of physical models more straightforward compared to the Eulerian framework where only moments of the probability density function are computed. Transport equations are then derived for the Lagrangian variables to track the spray's evolution during the simulation. Finally, a statistical weight is assigned to each numerical particle denoting the number of samples associated with each numerical particle to fulfill global constraints on mass, momentum and energy of the dispersed phase.

One major difficulty of this approach lies in the control of statistical convergence. For instance, zones depleted of numerical particles will induce non-physical oscillations of the dispersed phase fields when the latter are projected on the Eulerian grid.

(Garg 2009) proposed to locally seed the zones depleted of particles to circumvent this problem. Their main idea was to control the minimum and maximum number of particles in each computational cell. On the one hand, the numerical particles were split if the lower threshold value was reached to guarantee sufficient statistical sampling of the spray. On the other hand, the particles were gathered when the upper threshold was reached in order to limit oversampling and reduce computational expense. Consistency was ensured by respecting a constraint resulting from mass conservation and implying equality between the sums of particle weights before and after splitting / gathering. An important limitation of this approach lies in the arbitrary character of the threshold values.

The present paper proposes a possibly complementary approach to compensate the poor statistical convergence inherent to the Lagrangian approach. The main idea is to spread the information carried by each particle, initially strictly lo-

calized on each particle's center of gravity, over a finite distance. The associated length scale is approximately reconstructed via the resolution of additional transport equations for each particle. The fields resulting from the projection of Lagrangian variables on the computational mesh are then smoothed via the resolution of a nonlinear diffusion equation, approximately yielding a Gaussian smoothing of the initial particle fields.
The paper is organized as follows : section 2 reviews the governing equations for Euler-Lagrange approach. In section 3, the regularization procedure is introduced in two distinct steps : first, the reconstruction of the inter-particle distances. Then, the diffusion equation will be introduced. In section 4, the approach is evaluated on a 1D test case to prove its efficiency. The main findings of the present work are summarized in the conclusion.

2 Governing equations

Carrier phase

The present approach is restricted to steady carrier phases. Beyond this fundamental assumption, the system of equations that is solved for the carrier phase, i.e. incompressible / compressible Euler or Navier-Stokes equations, is irrelevant. Therefore, the set of equations for the carrier phase is not written in detail.

Dispersed phase

The spray is described using a probability density function (pdf) $f(t, \mathbf{x}, \mathbf{v})$ denoting the number of particles with position $\mathbf{x}$ and velocity $\mathbf{v}$ at time t. The evolution of f is given by the kinetic-like Williams equation (Williams 1958)

$$\frac{\partial f}{\partial t} + \nabla_{\mathbf{x}} \cdot (vf) + \nabla_{\mathbf{v}} \cdot (\gamma f) = 0 \tag{1}$$

with γ the acceleration rate. Note that eq. (1) describes a simplified version where fragmentation/coalescence and collision phenomena were discarded. These simplifications are mainly performed for preliminary studies and do not imply that the proposed methodology is restricted to sprays without fragmentation and coalescence phenomena.
A direct numerical resolution of Eq.(1) is not possible due to the size of the phase space. Thus, the Lagrangian approach is used to seek an approximation of f using a sample of N numerical particles. f is then approximated as:

$$f^N(t, \mathbf{x}, \mathbf{v}) = \sum_{p=1}^{N} w_p(t)\delta(\mathbf{x} - \mathbf{x}_p(t))\delta(\mathbf{v} - \mathbf{x}_p(t)) \tag{2}$$

with $\mathbf{x}_p$ and $\mathbf{v}_p$ the position and velocity of the particle p. w_p is a numerical weight that can be interpreted as the (not necessarily integer given the statistical nature of the sampling) number of real particles associated to the numerical particle p.

The idea of the present work is to view each particle as carrying information on the distance to its closest neighbour. Thus, each particle is now identified by its position, denoted $\bar{\mathbf{x}}_p$ and distance to the closest neighbouring particle $\mathbf{x}'_p$. We consider the spray to be initially properly sampled. Then, information on the evolution of the distance between two neighbouring particles along their trajectories may be gained if the evolution of $\mathbf{x}'_p$ can be tracked. This implies that two particles that were initially closest at injection remain close along their respective trajectories, requiring similar inertia. Evaluating $\mathbf{x}'_p$ explicitly could be complex in a parallel simulation environment as particles would have to be copied on adjacent processors to allow for the evaluation of $\mathbf{x}'_p$ across processor boundaries, as is done for instance for explicit evaluations of collisions (Capecelatro 2013). Thus, an approximate evolution equation for this distance is derived instead. This distance is then used to spread information carried by each particle over a characteristic distance proportional to $\mathbf{x}'_p$.

The initial position of each particle is decomposed as:

$$\mathbf{x}_p(t_0) = \bar{\mathbf{x}}_p(t_0) + \mathbf{x}'_p(t_0) \tag{3}$$

with $\mathbf{x}'_p(t_0) = \mathbf{x}_p(t_0) - \bar{\mathbf{x}}_p(t_0)$ to the closest neighbouring particle. Similarly, the particle velocity is defined as:

$$\mathbf{v}_p(t_0) = \bar{\mathbf{v}}_p(t_0) + \mathbf{v}'_p(t_0) \tag{4}$$

with $\bar{\mathbf{v}}_p(t_0)$ the initial velocity of the current particle and $\mathbf{v}'_p(t_0)$ the velocity of its neighbor.

The trajectories of the each numerical particle are given by the standard transport equations:

$$\begin{aligned} \frac{d\mathbf{v}_p}{dt} &= \boldsymbol{\gamma}_{\mathbf{p}} = \frac{1}{\tau_p}\left(\mathbf{u}(\mathbf{x}_p) - \mathbf{v}_p\right) + \mathbf{g} \\ \frac{d\mathbf{x}_p}{dt} &= \mathbf{v}_p \end{aligned} \tag{5}$$

with τ_p the particle time response given by the correlation ((Schiller and Naumann 1935))

$$\tau_p = \tau_0 \left(1 + 0.15 Re_p^{0.687}\right) \tag{6}$$

with $Re_p = \frac{d_p ||\mathbf{u}(\mathbf{x}_p) - \mathbf{v}_p||}{\nu}$ the particle Reynolds number and τ_0 the particle time response in the limit of zero particle Reynolds number.

3 Regularization procedure

Equation (2) implies that the pdf is only defined at positions where a numerical particle is present. The projection step on the Eulerian grid clearly leads to a regularization of eq. (2) because the Dirac delta function will at least be spread over the computational cell containing the particle. However, this regularization is mesh dependent so that the quality of the final solution may not be controlled. In particular, results obtained via projection on a finer grid while keeping the same initial sampling will tend to exhibit more non-physical oscillations. Moreover, in regions depleted of particles non-physical oscillations will inevitably appear on the dispersed fields. Instead of increasing the number of numerical samples/ particles in a static manner, i.e. by initializing with a higher number of samples, or in a dynamic fashion by

detecting the zones depleted of particles and increasing the seeding (Garg 2009), the present work proposes to regularize the Dirac delta function on the particle presence over a characteristic distance set by the evolution of the inner-particle distance. To this purpose, the Dirac distribution $\delta(\mathbf{x}-\mathbf{x}_p)$ appearing in Eq.(2) is regularized by a Gaussian distribution $\delta_{\sigma_p}(\mathbf{x}-\mathbf{x}_p)$ with the standard deviation σ_p controling the distance of the information spread around particle p. This regularization is based on the resolution of a diffusion equation. Indeed, applying a diffusion process over a time T to a Dirac distribution yields a Gaussian Distribution whose standard deviation σ is given by

$$\sigma = \sqrt{2DT} \tag{7}$$

This distance will be referred to as the regularization length scale for the rest of the paper. Intuitively, the standard deviation σ_p should be at least proportional according to the initial and to the evolution of the inner-particle distance to balance the poor particle resolution

$$\sigma_p = \sigma_p\left(\mathbf{x}'_p(t), \mathbf{x}'_p(t_0)\right) \tag{8}$$

where t_0 denotes the time of the initial condition.

However, this procedure can present three difficulties. First, the information on $\mathbf{x}'_p$ required to defined each σ_p is not available during the simulation since only the positions $\mathbf{x}_p$ of the particles are known. Although possible, an explicit evaluation of these distances may be expensive in a distributed memory environment. Therefore, an initial methodology to reconstruct these quantities is required.

Then, the methodology to replace Dirac distributions by Gaussian distributions presents two major constraints. First, the regularization length scale σ_p is specific to each particle and is thus expected to be a function of space. Again, performing the regularization explicitly is not straightforward in a parallel simulation environment, in particular when the regularization length scale extends over several grid cells.

The overall procedure proposed in this paper will be presented in two different steps : first, the methodology to approximately evaluate the evolution of the inner-particle distance, then the procedure to replace Dirac distributions by Gaussian distributions.

3.1 Reconstruction of $\mathbf{x}'_p$

The idea retained to reconstruct the values of $\mathbf{x}'_p$ is to design and solve transport equations similar to Eq.(5). These equations also stand for $\bar{\mathbf{x}}_p$

$$\begin{aligned}\frac{d\bar{\mathbf{v}}_p}{dt} &= \frac{1}{\tau_p}\left(\mathbf{u}(\bar{\mathbf{x}}_p) - \bar{\mathbf{v}}_p\right) + \mathbf{g}\\ \frac{d\bar{\mathbf{x}}_p}{dt} &= \bar{\mathbf{v}}_p\end{aligned} \tag{9}$$

Combining Eq.(5) and Eq.(9), one obtains

$$\begin{aligned}\frac{d\mathbf{v}'_p}{dt} &= \frac{1}{\tau_p}\left(\mathbf{u}(\mathbf{x}_p) - \mathbf{u}(\bar{\mathbf{x}}_p) - \mathbf{v}'_p\right)\\ \frac{d\mathbf{x}'_p}{dt} &= \mathbf{v}'_p\end{aligned} \tag{10}$$

Then, one assumes

$$\mathbf{u}(\mathbf{x}_p) - \mathbf{u}(\bar{\mathbf{x}}_p) \approx \nabla\,\mathbf{u}\cdot\mathbf{x}'_p \tag{11}$$

and the transport equations for $\mathbf{x}'_p$ finally write

$$\begin{aligned}\frac{d\mathbf{v}'_p}{dt} &= \frac{1}{\tau_p}\left(\nabla\,\mathbf{u}\cdot\mathbf{x}'_p - \mathbf{v}'_p\right)\\ \frac{d\mathbf{x}'_p}{dt} &= \mathbf{v}'_p\end{aligned} \tag{12}$$

It is recalled that this methodology is only applicable for steady fields of the carrier phase. Moreover, a stringent linearity assumption on the flow velocity in the neighbourhoud $\mathbf{x}'_p$ of a particle was made, see (Eq.(11)). The validity of such assumption may be controlled by evaluating the second derivatives of the carrier phase. In case this assumption becomes invalid, the flow field could be seeded with additional particles, as suggested by (Garg 2009).

3.2 Diffusion equation

The present section describes the implicit regularization procedure to approximately replace the Dirac delta functions on particle position by Gaussian distributions with a specific regularization length scale σ_p.
A similar method was introduced by (Poustis 2018) in the context of a deterministic discrete particle simulations in order to improve the robustness of numerical two-way coupling between the carrier phase and the spray. The method is based on the resolution of a non-linear diffusion equation

$$\partial_\tau\phi - \nabla\cdot\left(D\left(|\nabla\phi|^2\right)\nabla\phi\right) = 0 \tag{13}$$

It was shown in (Poustis 2018) that a diffusion coefficient expressed in terms of the gradient of the variable to regularize allowed to locally adjust the regularization length scale. However, this formulation can not directly be used in the present work because it is not adapted to varying numerical weights w_p. This is because the gradient function of the dispersed phase field is no longer uniquely defined with respect to the regularization length scale. Indeed, a large gradient of the considered dispersed phase field that is to be projected on the Eulerian grid could be induced by a small gradient multiplied by a large weight w_p or vice versa.
Since the regularization cannot be performed solving a single diffusion equation, the regularization is split in two successive steps. First, a field of diffusion coefficients that is nonzero not only in the computational cells containing the particles, but in a neighborhood defined by the magnitude of $\mathbf{x}'_p(t)$, needs to be defined. To this purpose, the Eulerian field of the characteristic diffusion length scale L_p is defined:

$$L_p(\mathbf{x};t) = \sum_{p=1}^{N}\mathbf{x}'_p(t)\;\mathbb{1}(\mathbf{x_p}(t),\mathbf{x}) \tag{14}$$

Then, a non-linear diffusion equation is applied to this

field:

$$\begin{aligned} \frac{\partial \psi}{\partial \tau} - \nabla \cdot (D(\psi) \nabla \psi) = 0, \mathbf{x} \in \Omega, \tau \in [0; \tau_{max}] \\ \psi(0, \mathbf{x}) = L_p(\mathbf{x}, t), \mathbf{x} \in \Omega \\ \frac{\partial \psi}{\partial n} = 0, \mathbf{x} \in \partial\Omega \end{aligned} \tag{15}$$

with a diffusion coefficient:

$$D(\psi) = \frac{2}{\pi} \arctan\left(\beta \left(\frac{\psi}{\psi_{\max}}\right)^{\alpha}\right), (\alpha, \beta) \in \mathbb{R}^{+} \tag{16}$$

Here, ψ denotes the regularized Eulerian inner-particle distance field. Taking a diffusion coefficient increasing with ψ allows to adjust the diffusion intensity according to the local inner-particle distance. This unsteady non-linear diffusion equation is solved over a non-physical pseudo-time τ_{max}. Although it is strictly speaking only valid in the case of linear diffusion, it appears eq. (7) remains approximately valid locally. Therefore, if the maximum value of the diffusion coefficient is arbitrarily set to unity, τ_{max} may be simply written as

$$\tau_{max} = \max_{p} \left|\left|\mathbf{x}'_p(t)\right|\right|^2 \tag{17}$$

This definition ensures that the largest inner-particle distance will be approximately spread over the correct length scale. A regularized inner-particle distance Eulerian field $\tilde{L}_p(\mathbf{x})$ is then obtained at the end of the first diffusion step:

$$\tilde{L}_p(\mathbf{x}) = \psi(\tau_{max}, \mathbf{x}) \tag{18}$$

Given this field of regularized length scales, the diffusion coefficient for the diffusion of the dispersed phase fields is simply defined as

$$\tilde{D}(\mathbf{x}) = k\, \tilde{L}_p^2(\mathbf{x}), k \in \mathbb{R}_{+} \tag{19}$$

and the regularized dispersed phase fields, typically particle density or particle velocity in the present case, writes

$$\begin{aligned} \frac{\partial \phi}{\partial \tau} - \nabla . \left(\tilde{D}(\mathbf{x}) \nabla \phi\right) = 0, \mathbf{x} \in \Omega, \tau \in [0; \tau_{max}] \\ \phi(0, \mathbf{x}) = v_p(\mathbf{x}, t), \mathbf{x} \in \Omega \\ \frac{\partial \phi}{\partial n} = 0, \mathbf{x} \in \partial\Omega \end{aligned} \tag{20}$$

Given the formulation of $\tilde{D}(\mathbf{x})$, the regularization time is set to $\tau_{max} = 1$.

3.3 Overall Strategy

The overall strategy to perform a Euler-Lagrange simulation using the regularization procedure proposed in the present study may be summarized as follows:

- First, solve the gaseous phase equations until steady state is reached.
- Then, solve the transport equations for the dispersed phase (eq. (5)). Also, solve the system of equations (12) as the first step of the regularization procedure.
- Solve the diffusion equation eq.(15) to set the diffusion coefficient field in the neighborhood of each particle according the computed inner-particle distance $\mathbf{x}'_p(t)$.
- Finally, apply the regularization procedure to any dispersed field (e.g. particle velocity field) by solving eq.(20).

4 Numerical methods

In this section, a brief overview of the numerical methods used to solve the different system of equations introduced in the previous sections is proposed.

The implementation of the regularization is targeted in the IGLOO2D 2D solver developped at ONERA for airfoil icing applications (Trontin 2017). In particular, the present regularization could improve the prediction of impinging particle mass fluxes on airfoil surfaces, a fundamental preliminary to the prediction of liquid deposition and subsequent ice accretion. Note that such regularization procedures are already used in practice when particle trajectories are computed with a Lagrangian approach, albeit in an empirical manner, i.e. with an arbitrary definition of the regularization length scales. Eulerian approaches do not suffer from these limitations since they directly transport averaged fields and because their resolution is based on the Eulerian grid. However, standard Eulerian methods are not able to handle the complex wall interaction dynamics occuring when ice crystals impinge and shatter on the airfoil. In that case, more than one particle velocity needs to be locally defined to correctly predict impingement dynamics and the resulting system of equations is difficult to solve in practice. Unfortunately, the implementation of the present regularization procedure is still ongoing and only results of simple one-dimensional simulations may be shown in the results section.

The resolution of the Lagrangian equations (12) is integrated with an explicit semi-analytical Euler scheme (Murrone 2011).
Moreover, the resolution of the two diffusion equations (eq. (15) and eq.(20)) is performed using a finite volume approach with explicit time integration. The time integration is restricted by a CFL condition on the time step $\delta\tau$

$$\delta\tau \leq \frac{\Delta x^2}{2 d D_{max}} \tag{21}$$

with d is the physical dimension of the problem, $D_{max} = \max(D)$ in the first diffusion problem and $D_{max} = \max(\tilde{D})$ in the second one. The explicit CFL is quite restrictive and an implicitation of the non-linear diffusion equations (eqs.20 and 15) is probably necessary to limit computational expense for realistic applications. Clearly, achieving an efficient resolution for these non-linear diffusion equations is an additional key aspect of the present methodology, but it is reported to future work and thus considered out of the scope of the present paper.

5 Results

5.1 Reconstruction of dispersed flow fields

This first test case is used to prove the ability of the regularization procedure to yield smooth dispersed fields.

A 1D domain is considered $[0; 40]$ with 401 discretization points. Initially, $n = 300$ particles ($w_p = 1$) are injected in a steady linear fluid $u(x) = x$ without initial velocity. The particles are carried by the fluid over a time T. The initial injection in space and the time T have been chosen to ensure there is approximately one particle per cell at the end of the simulation. Therefore, the initial injection of the particles is inhomogeneous and the inital values of $\mathbf{x}'_p(t_0)$ are also inhomogeneous. This allows to obtain smooth particle density and particle velocity fields, considered here as reference solutions.
The same simulation with the same parameters is repeated with $N = 75$ numerical particles with equal numerical weights ($w_p = 4$). Particle density and velocity fields are plotted against their respective reference solutions on Fig.(1) and (2). A zoom on the particle velocity field is displayed on Fig.(3) to highlight the oscillation phenomena. Given that for the reference solution, the injection is chosen to obtain one particle per cell, reducing the number of numerical particles automatically induces the apparition of oscillations on the dispersed fields.

In order to prove its capabilities, the regularization procedure introduced in the previous section is applied to these two fields. The results are split in two : first, the reconstruction of the inner-particle distance and then the regularization step.

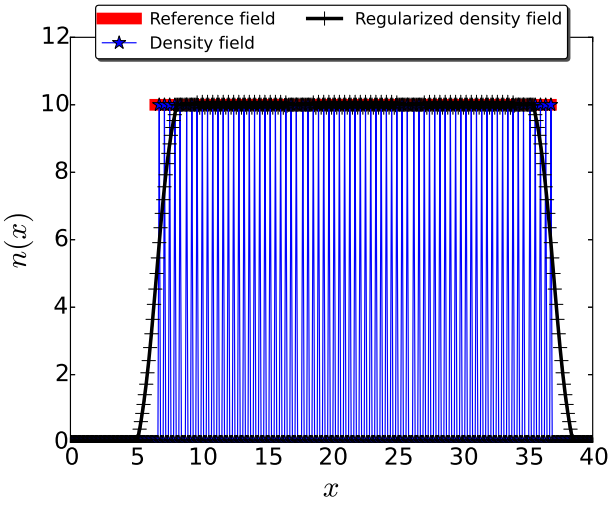

Figure 1: Comparison between the reference solution and the particle density field obtained with $N = 75$ numerical particles.

5.1.1 Reconstruction of $\mathbf{x}'_p$

In this simple case, the actual inner-particle distances can be measured in order to tune the procedure. The measured values are compared to the approximated values obtained by solving the transport equations (12). The simulation was

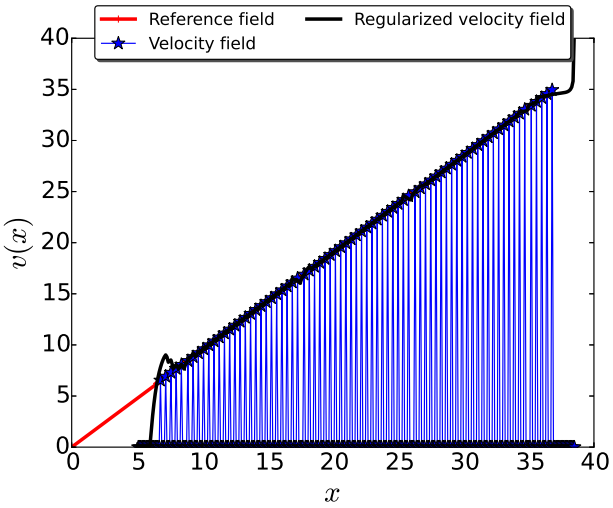

Figure 2: Comparison between the reference solution and the particle velocity field obtained with $N = 75$ numerical particles.

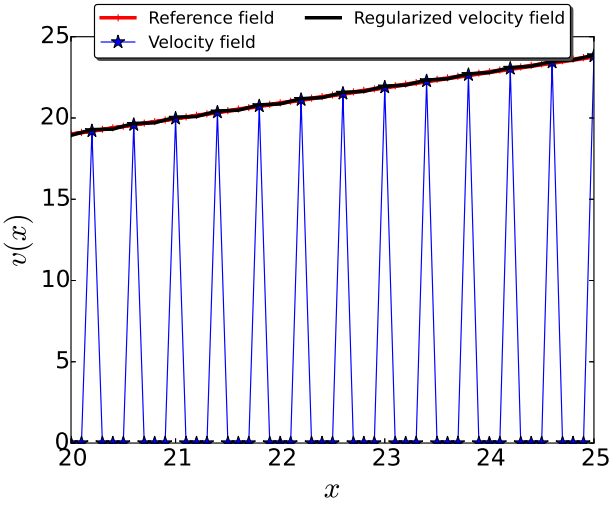

Figure 3: Zoom on the particle velocity field displayed in Fig.(2) to highlight the oscillation phenomena.

initialy performed with an equal and constant value of τ_p for all particles. In that case, the inner-particle distances were exactly reconstructed.
In real applications, the value of τ_p is given by eq.(6). In that case, the maximal error between the approximated and measured values is about $+9\%$, i.e. the reconstructed distances slightly overestimate the measured ones.

5.1.2 Regularization step

Then, the two diffusion equations are solved with initial conditions given by the non-regularized fields. The results are also displayed on Fig.(1) and Fig.(2). The resulting regularized fields accurately match the reference solutions except at the edge of the spray where some discrepancies can be noticed.

In an effort to provide a quantitative information about this procedure, the previous simulation was repeated for different

numerical particles number N with the regularization procedure to obtain a smooth particle velocity field in each simulation. Then, the error made is evaluated via a relative L^2 norm error between the reference solution and the regularized particle velocity field in each simulation. The errors obtained are displayed in Table.(1) for their corresponding number N of numerical particles normalized by the initial number $n = 300$ of real particles.

N/n	$\left(\frac{\|\|v_{ref}(\mathbf{x})-v_p(\mathbf{x})\|\|^2}{\|\|v_{ref}(\mathbf{x})\|\|^2}\right)^{1/2}$
0.125	$7.0.10^{-3}$
0.25	$4.6.10^{-3}$
0.50	$3.8.10^{-3}$
0.75	$1.3.10^{-3}$

Table 1: Relative L^2 norm error between the reference solution and the regularized particle velocity fields for different initial number of numerical particles .

The results obtained are again quite acceptable even for the worst case scenario $N/n = 0.125$.
Regarding the overal computational cost of the regularization procedure, the time required is not necessarily meaningful here in a fictive 1D test case. It will be more interesting to measure this cost on a more realistic 2D case. However, in order to simply give an order of magnitude, the resolution of the two diffusion equations required approximately 50 iterations in time. Thus, the regularization procedure is only applicable for post-processing purposes in its current form, typically for the reconstruction of particle mass flux profiles on an airfoil.

5.1.4 Non-constant numerical weight

It was previously mentioned that difficulties could occur when dealing with particles having different numerical weights w_p. In order to check the robustness of our methodology, the previous simulation was repeated using numerical particles with varying numerical weight w_p. The same parameters than the previous test case are used and the numerical weight of each particle is randomly picked between 1 and 10. The number of real particle represented is therefore randomly sampled. The error made on the reconstruction of the inner-particle distance is identical to the case with constant numerical weight since the numerical weights are not involved in the reconstruction. Concerning the regularization, the results obtained are plotted with the reference solution on Fig.(4) and are still in good agreement.

5.1.5 Non-Linear velocity profile

One major assumption made in the derivation is to assume a linear flow field over the distance separating neighboring particles. The finite distance for each particle is given by $\mathbf{x}'_p$. When this assumption is no longer verified, the error done on the reconstruction of the inner-particle distances is significantly increased. Therefore, the present procedure would need to be combined with a seeding procedure when the linearity assumption is locally violated over the computed regularization distance. For the moment, only a criterion that should detect departure from linearity is proposed.

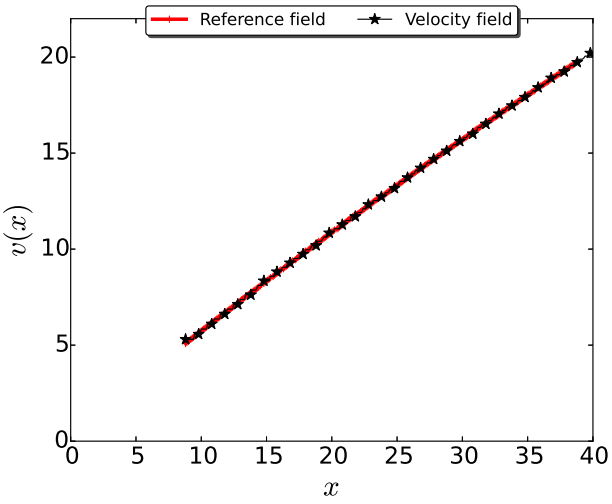

Figure 4: Regularized particle velocity field with non-constant numerical weights. Comparison with the reference solution.

$$\left|\frac{1}{2}\Delta u(\mathbf{x}_p(t))x_p^{'2}\right| \leq \epsilon\,|u(\mathbf{x}_p(t))| \tag{22}$$

with ϵ a constant of order 10^{-2}.

6 Conclusions

In this paper, a methodology to improve the statistical convergence of the Euler-Lagrange approach for dispersed two-phase flows simulations is proposed. Dispersed fields are regularized/smoothed via the resolution of a diffusion equation. The regularization length scale is based on the inner-particle distance. Since these distances are not available nor measurable during the simulation, a prior methodology to approximately reconstruct this information is proposed. The methodology proved to be able to obtain smooth particle velocity field on a fictive 1D test case. The influence of the initial number of numerical parameters and then the influence of non-constant numerical weights on the quality of the projected Lagrangian fields were tested. In both cases, the results were in good agreement with reference solutions obtained with much higher initial particle seeding.
The next step will be to evaluate this methodology on a more representative 2D test case in the context of icing applications. A comparison between different methods to achieve convergence for particle mass flux fields on standard airfoils will then be performed. First, convergence mass deposition rates will be achieved via static seeding, i.e. increasing the initial number of injected particles. Then dynamic seeding, where the number of particles present in each cell is controlled via minimum and maximum threshold values. Finally, the present methodology will be used. The computational expense of these and their respective average error levels with respect to a reference solution may then be compared.

References

Crowe, C., Sharma, M.P. & Stock, D.E. The Particle-Source-In Cell (PSI-CELL) Model for Gas-Droplet Flows. J. of Fluids Engineering, Vol. 99(2) pp. 325-332 (1977)

Poustis, J.-F., Senoner, J.-M., Zuzio, D. & Villedieu, P. Regularization of the Lagrangian point force approximation for deterministic discrete particle simulations, in preparation for International of Multiphase Flow

Williams, F. Spray combustion and atomization. Phys. of Fluids 1 (6) pp. 541-545(1958)

Garg, R., Narayanan, C., & Subramaniam, S. A numerically convergent Lagrangian Eulerian simulation method for dispersed two-phase flows. Int. J. of Multiphase Flow, 35(4), pp 376-388 (2009)

Zuzio, D., Thuillet, S., Senoner, J.-M., Laurent, C., Rouzaud, O., Gajan, P. Multi-solver LES simulation of the atomization on a cross-flow liquid jet in a channel. INCA Workshop (2017)

Schiller, L., Naumann, Z. A drag coefficient correlation. Z. Ver. Deutsch. Ing, 77(1):318-320, 1935

Trontin, P., Blanchard, G., Kontogiannis, A., & Villedieu, P. (2017). Description and assessment of the new ONERA 2D icing suite IGLOO2D. In 9th AIAA Atmospheric and Space Environments Conference (p. 3417).

Murrone, A., & Villedieu, P. (2011). Numerical modeling of dispersed two-phase flows. AerospaceLab, (2), p-1.

Capecelatro, J., & Desjardins, O. (2013). An Euler-Lagrange strategy for simulating particle-laden flows. Journal of Computational Physics, 238, 1-31.